

OCELLI: TRANSIENT DISEQUILIBRIUM FEATURES IN A LOWER CARBONIFEROUS MINETTE NEAR CONCORD, NORTH CAROLINA

RICHARD L. MAUGER

Department of Geology, East Carolina University, Greenville, North Carolina 27858, U.S.A.

ABSTRACT

The lower Carboniferous Concord minette in North Carolina contains coarse phlogopite ($Mg^* = 0.9$; some is deformed), finer size phlogopite ($0.9 < Mg^* < 0.4$) that grew *in situ*, abundant carbonates (15 vol. %), and lacks clinopyroxene. Spherulitic groundmass sanidine and albite show that the dyke cooled quickly. Ti distributions in phlogopite indicate emplacement temperatures of 1050–1100°C, and lack of annealing in deformed phlogopite suggests rapid ascent of the magma. The dyke contains carbonate-dominant (CDO) and feldspar-dominant (FDO) ocelli. The CDO grew as immiscible carbonate-melt droplets in the dyke. Of possible origins for the FDO, only the crystallization of silicate solute droplets condensed from dense fluid-phase bubbles is viable. Rapid decompression, as the magma rapidly rose from mantle or lower crustal depths, generated strong simultaneous oversaturations in fluids ($H_2O + F$) and carbonates. Dissolved carbonates lowered fluid solubilities, allowing for fluid-phase oversaturations with relatively small fluid contents ($H_2O + F \leq 3$ wt. %) in the magma. High diffusivities for alkalis, H_2O , and F promoted rapid growth of the fluid-phase bubbles while OH^- and F^- solubilities in the magma were still suppressed by dissolved carbonates. As the carbonates slowly exsolved, fluid solubilities gradually rose, and the fluid-phase H_2O and F redissolved in the magma. Condensed silicate solute from the bubbles remained as compositionally distinct droplets (mostly normative alkali feldspars and minor quartz, devoid of MgO) embedded in the magma. Rapid cooling preserved the droplets as the FDO. Phlogopite halos surrounding both kinds of ocelli originated through enhanced nucleation and grain growth in the bubble-melt interfacial zone where melt polymerization was locally lowered by H_2O from the bubbles redissolving in the melt. Larger FDO (>3 mm in dia.) without halos represent condensed solute from vesicles in the hottest part of the dyke where the vesicles redissolved before the *in situ* phlogopite began to nucleate. Segregation vesicles in deep-sea basalts may originate via a similar mechanism. Early water-rich vesicles are diluted by more slowly exsolving CO_2 , causing the silicate solute to condense in the vesicles. Rapid cooling preserves the solute as felsic glass in the vesicle. An origin for segregation vesicles via late-stage, porous-media flow is flawed by the extremely low permeabilities involved and by a requirement for high pressure gradients to push the interstitial melt toward the vesicles.

Keywords: minette, emplacement temperature, ocelli, carbonate, feldspar, fluid phase, solubilities, disequilibrium, vesicles, theory of formation, lower Carboniferous, Concord, North Carolina.

SOMMAIRE

La minette de Concord, en Caroline du Nord, d'âge carbonifère inférieur, est composée de phlogopite à grains grossiers ($Mg^* = 0.9$) dont certains sont déformés, de phlogopite à grains plus fins ($0.9 < Mg^* < 0.4$) qui ont cristallisé *in situ*, et une abondance de carbonates (15% par volume); par contre, le clinopyroxène est absent. Un amas sphérolitique de sanidine et d'albite dans la pâte témoigne d'un refroidissement rapide. La teneur en Ti de la phlogopite indique une température de mise en place de 1050–1100°C; l'absence de recristallisation dans les cristaux déformés indique une mise en place rapide du magma. Le filon contient deux sortes d'ocelli, à dominance de carbonates ou de feldspaths. Les ocelli carbonatés représentent des gouttelettes d'un liquide carbonaté immiscible. Parmi les hypothèses envisagées pour expliquer la formation des ocelli à feldspaths, seule celle de la cristallisation d'un soluté condensé à partir de bulles d'une phase gazeuse dense est satisfaisante. Une décompression rapide au cours de la montée du magma d'une source située dans le manteau ou dans la croûte provoque une sursaturation simultanée en phase gazeuse ($H_2O + F$) et en carbonates. La fraction carbonatée dissoute abaisse la solubilité des gaz dans le magma, et peut ainsi causer une sursaturation en gaz, même avec une teneur relativement faible de $H_2O + F$ dans le magma (< 3% en poids). Une diffusivité élevée des alcalins, H_2O et F permet un accroissement rapide des bulles pendant que la solubilité de OH^- et de F^- est encore faible, les carbonates étant dissouts. Avec l'exsolution progressive de ces carbonates, la solubilité des fluides augmente peu à peu, et les composants H_2O et F sont redissouts dans le magma. Le soluté silicaté condensé des bulles reste sous forme de globules de composition distincte dans le magma (feldspaths prédominants, avec un peu de quartz, mais sans Mg), préservés à la suite de la trempe. La gaine de phlogopite autour des deux sortes d'ocelli résulte d'une nucléation plus facile et d'une croissance accrue de cristaux à l'interface entre le liquide silicaté et la bulle, dues à l'abaissement local du degré de polymérisation par l'eau de la bulle dissoute dans le magma. Les ocelli feldspathiques plus gros (plus de 3 mm de diamètre), sans gaine, représenteraient un soluté condensé à partir de bulles dans la partie du filon à la température la plus élevée, dans laquelle les bulles sont résorbées avant la nucléation de la phlogopite. Les ségrégations dans les vacuoles des basaltes marins pourraient avoir une origine semblable. Des bulles précoces, riches en H_2O , sont diluées à cause de l'exsolution plus lente du CO_2 , ce qui mènerait à la condensation d'un soluté enrichi en silicates. Un refroidissement rapide conserve le soluté sous forme de verre siliceux dans la vacuole. Une autre hypothèse, celle de circulation tardive en milieu poreux, est jugée inaccép-

table vues les perméabilités extrêmement faibles et les gradients de pressions trop élevés requis pour forcer la fraction liquide interstitielle dans les vacuoles.

(Traduit par la Rédaction)

Mots-clés: minette, température de mise en place, ocelli, carbonate, feldspath, phase gazeuse, solubilité, déséquilibré, vacuole, théorie de formation, carbonifère inférieur, Concord, Caroline du Nord.

INTRODUCTION

Lower Carboniferous minette dykes (Table 1) intrude plutonic and meta-igneous rocks of the Charlotte Belt near Concord and Harrisburg, North Carolina (Fig. 1) (Bell & Overstreet 1959). Fresh

minette (named the Concord minette) from a dyke that intruded Concord syenite southwest of Concord (Fig. 1) contains abundant alkali feldspar (50 vol. %), phlogopite (33 vol. %), carbonates (15 vol. %), and minor quartz. Clinopyroxene is conspicuously absent. The Concord minette also contains feldspar-dominant and carbonate-dominant ocelli. A distinctive halo of tangential phlogopite flakes surrounds all ocelli except for the largest feldspar-rich variety.

Some minettes elsewhere have been emplaced at high temperatures ($T > 1000^{\circ}\text{C}$) after rapidly rising from lower crustal or greater depths (Mercier 1979, Ehrenberg 1979, Esperanca & Holloway 1987). Rapid decompression and cooling provide the physicochemical framework for studying the ocelli and other textural features in the Concord minette. I will argue that the ocelli represent quenched products of transient disequilibrium processes operating in the dyke magma; decompression caused the disequilibrium conditions and rapid cooling preserved the disequilibrium features.

PHLOGOPITE TEXTURES AND COMPOSITIONS

Biotite in the Concord minette varies in grain size, composition, and texture. Small randomly-oriented flakes (< 0.5 mm) predominate (22 vol. %) (Fig. 2E, J). Grain size gradually increases toward the center of the dyke. These grains have a light-tan phlogopitic core and a nearly opaque Fe-rich overgrowth crowded with apatite (Fig. 2A, E, I, J). The small matrix flakes mimic plagioclase laths in an intergranular texture, suggesting *in situ* growth in a sta-

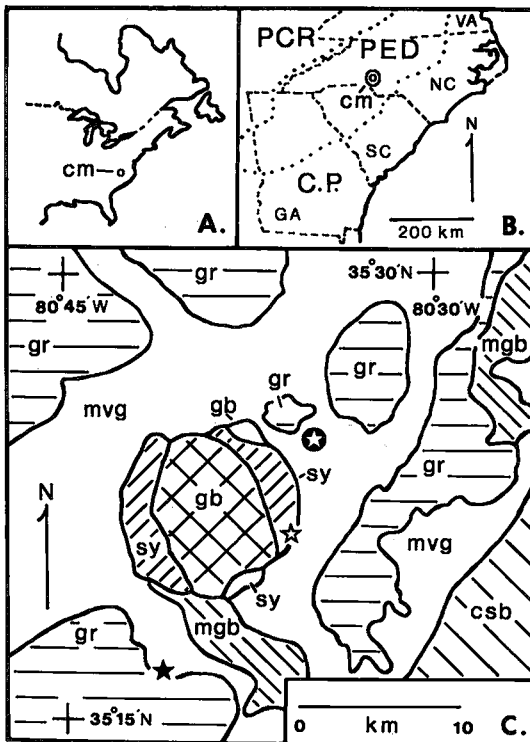


Fig. 1. Location and geological map, Charlotte Belt minettes. Cm (minette localities), PCR (Paleozoic Craton), PED (Piedmont), Paleozoic and Precambrian crystalline rocks), C.P. (post-Paleozoic Atlantic Coastal Plain sediments), open star (Concord minette), black star (Harrisburg minettes), and open star in black circle (city of Concord, NC): Map legend: *Charlotte Belt* gr — 300 to 400 Ma granites; sy (syenite), gb (gabbro), mgb (metagabbro) — Concord plutonic suite (415 Ma); mvg — metavolcanics and gneisses, late Precambrian to Cambrian; *Carolina Slate Belt* (csb). Geology generalized from Goldsmith *et al.* (1978).

TABLE 1. K-AR DATA FOR CONCORD AND HARRISBURG MINETTES AND CONCORD SYENITE

	K%	^{40}Ar rad pm/g	^{40}Ar atom%	Age Ma
Cm phlogopite UAKA 82-161	7.461 (0.042) "7"	4788 (12) "4"	0.8 (0.1) "4"	337 +8
Cm sanidine* UAKA 82-161	5.926 (0.005) "5"	3936 (7) "6"	1.9 (0.8) "6"	347 +8
Csy biotite UAKA 85-72	7.052 (0.076) "3"	5932 (15) "5"	1.3 (0.1) "5"	430 +10
Hm phlogopite UAKA 84-139	7.778 (0.038) "4"	4904 (8) "4"	0.9 (0.06) "4"	331 +8

means underlined; one s.d. in parentheses; number of determinations in quotation marks; analyses from Lab. Isotope Geochem., Univ. of Arizona.

Cm — Concord minette
Csy — Concord syenite
Hm — Harrisburg minette

35° 21.03'N, 80° 36.22'W

0.4 km N. of UAKA 82-161

35° 16.29'N, 80° 40.32'W

$$\lambda_{\beta} = 4.963 \times 10^{-10} \text{ yr}^{-1} \quad \lambda_{\epsilon} = 0.581 \times 10^{-10} \text{ yr}^{-1}$$

$$^{40}\text{K}/\text{K} = 1.167 \times 10^{-4} \text{ atom/atom}$$

sanidine*: contains some albite and quartz

tionary magma (Fig. 2E). The light-tan cores have fairly high Mg* (0.7 to 0.9; Mg/Mg + Fe, atomic), but Cr₂O₃ is generally less than 0.1%. The dark overgrowths (battlemented ends; Williams *et al.* 1982) are rich in Fe, Ti, and Ba, contain Mn (0.1% MnO), and are depleted in F (Table 2).

The much coarser phlogopite phenocrysts (1 to 5 mm; 11 vol%) as in minettes elsewhere (Reynolds 1931, Roden & Smith 1979) are generally aligned parallel to the dyke walls. However, local eddy-like phenocryst patterns suggest penetrative flow during dyke emplacement. Some larger phenocrysts are kinked or bent (Fig. 2A) and may show anomalous birefringence patterns (visible near extinction). These deformations involve intracrystalline slip on {001} (Nicolas & Poirier 1976). The smaller matrix flakes are not deformed. Larger phenocrysts may have dark altered zones along cleavage traces (Fig. 2P). The phenocrysts are light tan and Mg*s are consistently about 0.9; Cr, Ni, and F are enriched and Ti and Ba are depleted. Red-brown zones are higher in Ti, Ba, and Fe but depleted in Cr, Ni, and F (Table 2).

Probably-cognate xenoliths (<3 mm) in the minette consist of phlogopite, alkali feldspar, and minor rutile. The xenolithic phlogopite is typically embayed (Fig. 2R) and shows minor kinking and other evidence for deformation. Light-tan cores have Mg*, Ni, Cr, and F contents similar to the phenocrysts (Table 2), but most grains have darker rims. A few grains with {001} edges impinging on rutile are dark reddish brown and enriched in Ti (Table 2, analysis 9). These Ti-rich zones may be diffusion halos (LeCheminant & LeCheminant 1985). The rutile contains FeO (about 2 wt. %) as its major impurity; opaque rims are richer in FeO and may include titanite and an Fe-Ti oxide as alteration products. Alkali feldspars in the xenoliths exhibit a microgranophyric texture in contrast to the spherulitic habit of the matrix feldspars (Fig. 2R; compare with Fig. 2B,C).

Minor pale green siliceous phlogopite (Table 2, anal. 14) occurs in carbonate-dominant ocelli and as an alteration product of olivine. Reversely pleochroic biotite (Farmer & Boettcher 1981) was not observed. Compositions and compositional zoning trends are similar to those reported from other minettes (Ehrenberg 1979, Bachinski & Simpson 1984, LeCheminant & LeCheminant 1985).

PSEUDOMORPHS AND XENOLITHIC FRAGMENTS

Aggregates of calcite, chlorite, hematite, quartz, siliceous phlogopite, and minor barite and celestine are interpreted as pseudomorphs after olivine (Fig. 2C). Talc, a common alteration product of olivine in minettes, was not recognized. Smaller tabular pseudomorphs of very fine-grained calcite (Fig. 2C)

probably altered from small groundmass clinopyroxene crystals. The Concord minette also contains rare fragments of vein-type quartz.

TABLE 2. CHEMICAL COMPOSITIONS* OF CONCORD MINETTE PHLOGOPITE AND BIOTITE

	1	2	3	4	5
SiO ₂	39.98	40.60	39.93	39.55	38.68
TiO ₂	3.52	2.94	3.24	4.17	4.76
Al ₂ O ₃	14.21	14.12	14.22	14.58	13.39
FeO _t	4.46	4.09	3.89	6.54	11.29
MgO	21.90	22.46	20.59	20.61	17.13
MnO	0.05	0.04	0.04	0.06	0.10
CaO	0.04	0.03	0.03	0.05	0.10
Na ₂ O	0.19	0.12	0.16	0.37	0.28
K ₂ O	9.66	9.84	9.93	9.01	8.63
F	1.28	1.29	1.42	1.32	0.83
Cl	0.02	0.02	0.03	0.02	0.02
BaO	0.46	0.37	0.36	0.73	0.92
Cr ₂ O ₃	0.74	1.84	1.16	0.16	0.03
NiO	0.29	0.40	0.42	0.20	0.08
O = F,Cl	0.55	0.54	0.60	0.56	0.35
Total	96.25	97.62	94.82	96.81	95.89

	6	7	8	9	10
SiO ₂	40.28	40.33	39.88	38.66	41.16
TiO ₂	3.38	3.27	4.42	6.62	3.65
Al ₂ O ₃	14.28	13.84	14.41	15.30	13.44
FeO _t	4.36	4.77	4.50	4.72	5.61
MgO	21.80	22.72	21.43	19.13	22.37
MnO	0.04	0.04	0.05	0.04	0.04
CaO	0.04	0.05	0.04	0.04	0.04
Na ₂ O	0.15	0.25	0.15	0.18	0.21
K ₂ O	9.68	9.46	9.51	9.59	8.89
F	1.34	1.44	1.12	0.97	1.20
Cl	0.02	0.02	0.02	0.02	0.01
BaO	0.41	0.58	0.52	0.64	0.51
Cr ₂ O ₃	0.95	0.28	0.78	0.35	0.10
NiO	0.30	0.18	0.28	0.19	0.12
O = F,Cl	0.61	0.61	0.48	0.41	0.51
Total	96.42	96.62	96.63	96.04	96.84

	11	12	13	14
SiO ₂	39.58	35.19	36.00	42.74
TiO ₂	5.20	6.84	5.89	0.88
Al ₂ O ₃	14.57	14.74	14.88	11.49
FeO _t	15.05	19.39	17.73	8.83
MgO	11.70	9.72	11.24	21.65
MnO	0.10	0.16	0.13	"0"
CaO	0.07	0.07	0.10	0.11
Na ₂ O	0.39	0.18	0.18	0.15
K ₂ O	8.56	8.84	8.78	9.00
F	0.58	0.37	0.38	1.29
Cl	0.04	0.05	0.05	"0"
BaO	1.37	1.80	1.68	"0"
Cr ₂ O ₃	0.03	0.05	0.06	"0"
NiO	0.13	0.12	0.13	nd
O = F,Cl	0.25	0.17	0.17	0.53
Total	97.12	97.35	97.06	95.61

* electron microprobe data; "0" means sample cts. exceed background cts. or s.d. exceeds 40%; nd means not determined; see Solberg & Speer (1982) for analytical details.

Sample Descriptions, Mg* in Parentheses

1. Ave. of 10 interior points in coarse phlogopite (0.90).
2. Ave. of 6 interior high-Cr analyses in a coarse phlogopite (0.91).
3. Alteration zone, interior of coarse phlogopite (0.90).
4. Dark red-brown interior zone in light-tan coarse phlogopite (0.73).
5. Dark red-brown interior zone in light-tan coarse phlogopite (0.90).
6. Interior point, light-tan coarse phlogopite (0.90).
7. Low-Ti and low-Cr analysis of light-tan coarse phlogopite near edge of grain (0.90).
8. Light-tan phlogopite from cognate xenolith (0.90).
9. Dark red-brown phlogopite (in Ti diffusion halo) in contact with rutile in cognate xenolith (0.88).
10. Interior analysis of light-tan in situ phlogopite (0.88).
11. Dark tip of in situ flake (0.58).
12. Dark tip of in situ flake (0.53).
13. Very dark nearly opaque tip of in situ flake (0.47).
14. Pale-green siliceous phlogopite from carbonate-dominant ocellus (0.81).

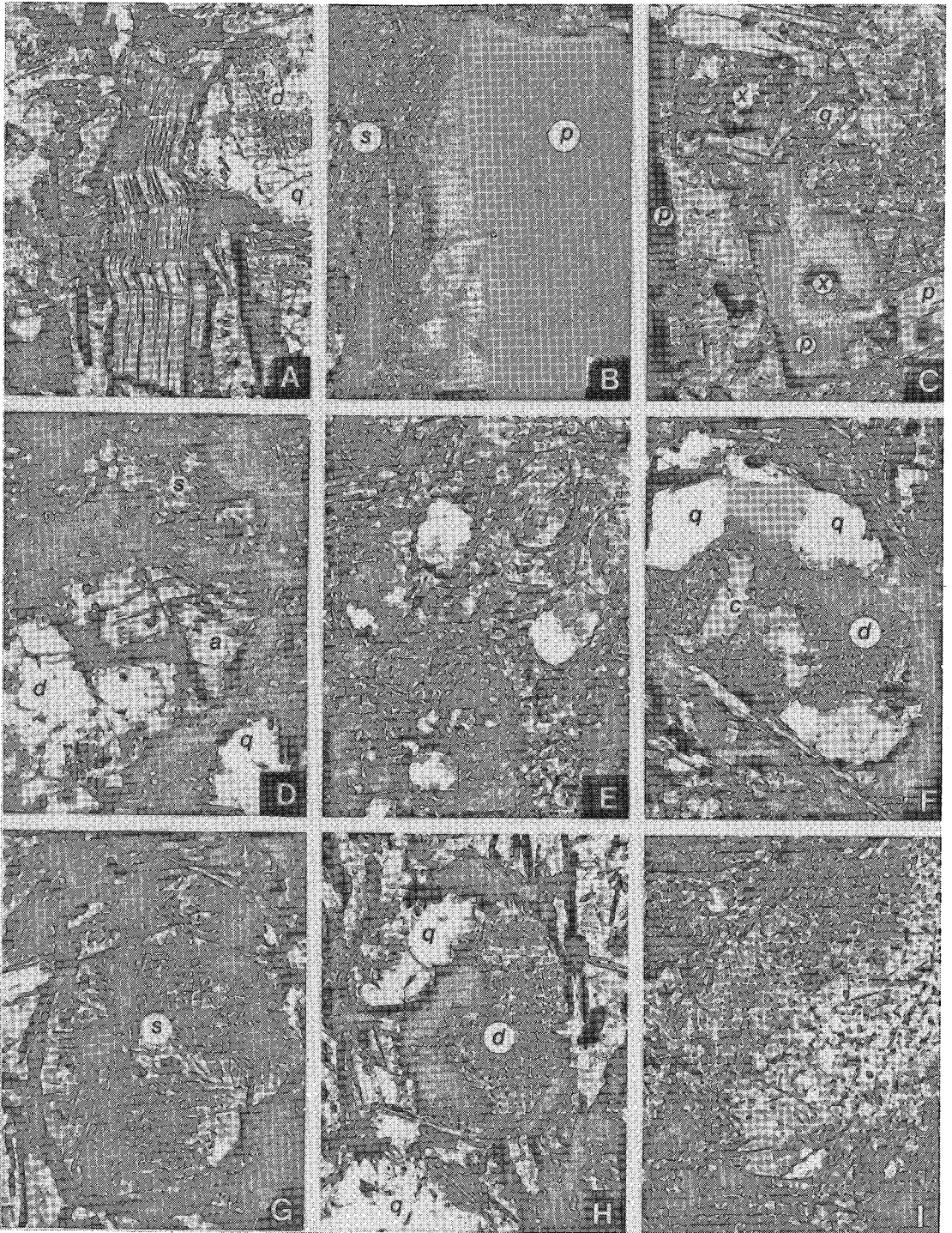


FIG. 2. Photomicrographs of the Concord minette. Long dimension of each photo is given in parentheses at the end of explanation. Minerals are labeled as follows: albite (a); calcite (c); dolomite (d); granular calcite pseudomorph after clinopyroxene (g); phlogopite (p); quartz (q); sanidine (s); and pseudomorph after olivine (x). A. Kinked phlogopite phenocryst and CDO with phlogopite halo. Matrix is spherulitic sanidine, phlogopite, and cpx-pseudomorphs;

MATRIX TEXTURES

Near the dyke margins, the Concord minette exhibits an orb texture (not to be confused with orbicular texture; Lofgren 1971b, Carstens 1982) in which small pebble-size spherulitic sanidine orbs are set in an albite matrix (Fig. 3). The sanidine orbs are compound spherulitic clumps that grew before the remaining glass, enriched in Ab and greatly depleted in Or, subsequently crystallized as albite. The sanidine orbs never impinged, so their globular shape was retained. The orb texture becomes less distinct and disappears toward the center of the dyke. The albite content of the rock also gradually decreases inward as continuous matrix albite gradually gives way to isolated albite clumps enclosed by sanidine. The spherulites consist of clouded, inclusion-riddled sanidine fibers (<5µm in cross section; feldspar determined as sanidine using 3-peak method of Wright 1968) and minor quartz slivers (Fig. 2C, D). Albite forms microgranophric aggregates and spherulitic clumps, also with minor quartz (Fig. 2M). Microprobe analyses typically gave nearly pure Or and Ab end-member compositions; rare intermediate compositions probably resulted from analyzing sanidine-albite mixtures. The average sanidine (Or 97.6) is typically richer in Ca (0.12% CaO), Fe (0.3% FeO), and Ba (0.4% BaO) than the average albite (Ab 99.3; 0.05% CaO, 0.1% FeO, and BaO <0.1%). Other matrix phases include carbonates, pyrite, a dark unidentified microdendritic phase, and tiny apatite crystals (Fig. 2B). The apatite contains small amounts of Sr (1% SrO), S (0.5%), Cl (0.2%) and LREE (0.1 to 0.2% La, Ce, and Nd as oxides).

OCELLI IN THE CONCORD MINETTE

In common with minettes and other lamprophyres (Roedder 1979, Carmichael *et al.* 1974, Cooper 1979, Carstens 1982, Rock 1984), the Concord minette contains ocelli (Fig. 2). They are fairly abundant (<10 vol.%) in a few thin sections, but make up only a tiny fraction of the dyke. Some ocelli consist mainly of carbonates (designated as CDO for carbonate-

dominant ocelli), others are mainly alkali feldspar (designated as FDO for feldspar-dominant ocelli, Fig. 2E, I, J), and a few contain carbonates and feldspars as major components (Fig. 2D, K). The ocelli increase in size and decrease in abundance from the walls toward the center of the dyke. The largest FDO occur only in the central part of the dyke. They typically contain quartz and minor carbonates (Fig. 2G, J). The CDO also contain quartz, but alkali feldspar is lacking or present in very small quantities (Fig. 2F, H, L, Q).

The FDO are conspicuously devoid of phlogopite. Most FDO consist of sanidine (Fig. 2G), a few are albite, and others include both feldspars (Fig. 2D). Spherulite and grain morphologies are similar to those of the respective matrix feldspars. The spherulitic sanidine clumps impinge in the centers of the ocelli and the crystals diverge inward, showing that grain growth proceeded inward from the ocelli walls. The nearly equidimensional crystals in the ocellar albite (Fig. 2M) suggest nucleation at multiple random sites inside the ocelli (Phillips 1973). Most FDO contain one or more euhedral to subhedral single-crystal quartz grains that also grew from the walls inward. Highly acicular, skeletal, or chain-like crystals of biotite occur only in the largest FDO (Fig. 2I). Other minor phases include carbonates, pseudomorphs after clinopyroxene, dark unidentified microdendrites intergrown with the feldspar (Fig. 2G), and pyrite that grew on the ocelli walls or along arcuate surfaces inside the ocelli (see Cooper 1979, Fig. 7).

Small- to medium-size ocelli (0.5 to 3 mm) are most abundant. Many have a halo of tangential phlogopite flakes (Read 1926, Rock 1984) (Fig. 2). Low sphericities and locally crinkled rims (Fig. 2D, E, G, J, K) suggest minor deformation and shrinkage (see also Phillips 1973). The large ocelli (3 to 6 mm) have a poorly developed halo or lack one entirely (Fig. 2I). Acicular biotite crystals and cpx-pseudomorphs are common only in the outer parts of these larger ocelli (Fig. 2I). FDO may contain smaller CDO (Fig. 2K) but the CDO never contain smaller FDO.

needle-like prisms (upper-left) are apatite (3.1 mm). B. Apatite in dark overgrowth rim on phlogopite phenocryst. Matrix apatite is intergrown with spherulitic sanidine (0.5 mm). C. Pseudomorphs after olivine and clinopyroxene. Matrix is spherulitic sanidine (0.5 mm). D. Portion of mixed ocellus with crinkled rim. Note spherulitic to microgranophytic albite aggregates, the microdendritic phase (biotite?) and the angular original pore now filled with quartz at lower-right (1.2 mm). E. Ocelli with phlogopite halos. Note the sanidine (grey), carbonates and quartz (clear grains), the acicular phlogopite in the larger FDO, and the large FDO (upper-right) that lacks a well developed phlogopite halo (6.9 mm). F. CDO. Note the pyrite (opaque grains in ocellus) and the phlogopite halo (1.2 mm). G. FDO with crinkled rim. Note the microdendritic phase, spherulitic sanidine, the phlogopite halo, the acicular phlogopite (upper-left part of ocellus), and the euhedral opaque grains of pyrite in the ocellus (1.2 mm). H. CDO with crinkled rim. Note hematite (opaque grains in ocellus), chlorite-calcite aggregate (left-center of ocellus), quartz-filled pore (lower left), and matrix sanidine (1.2 mm). I. Portion of large FDO. Ocellus lacks phlogopite halo; ocellar phases include sanidine (grey), quartz (clear), acicular phlogopite, and cpx-pseudomorphs as small, equidimensional dark-gray to black grains (6.9 mm).

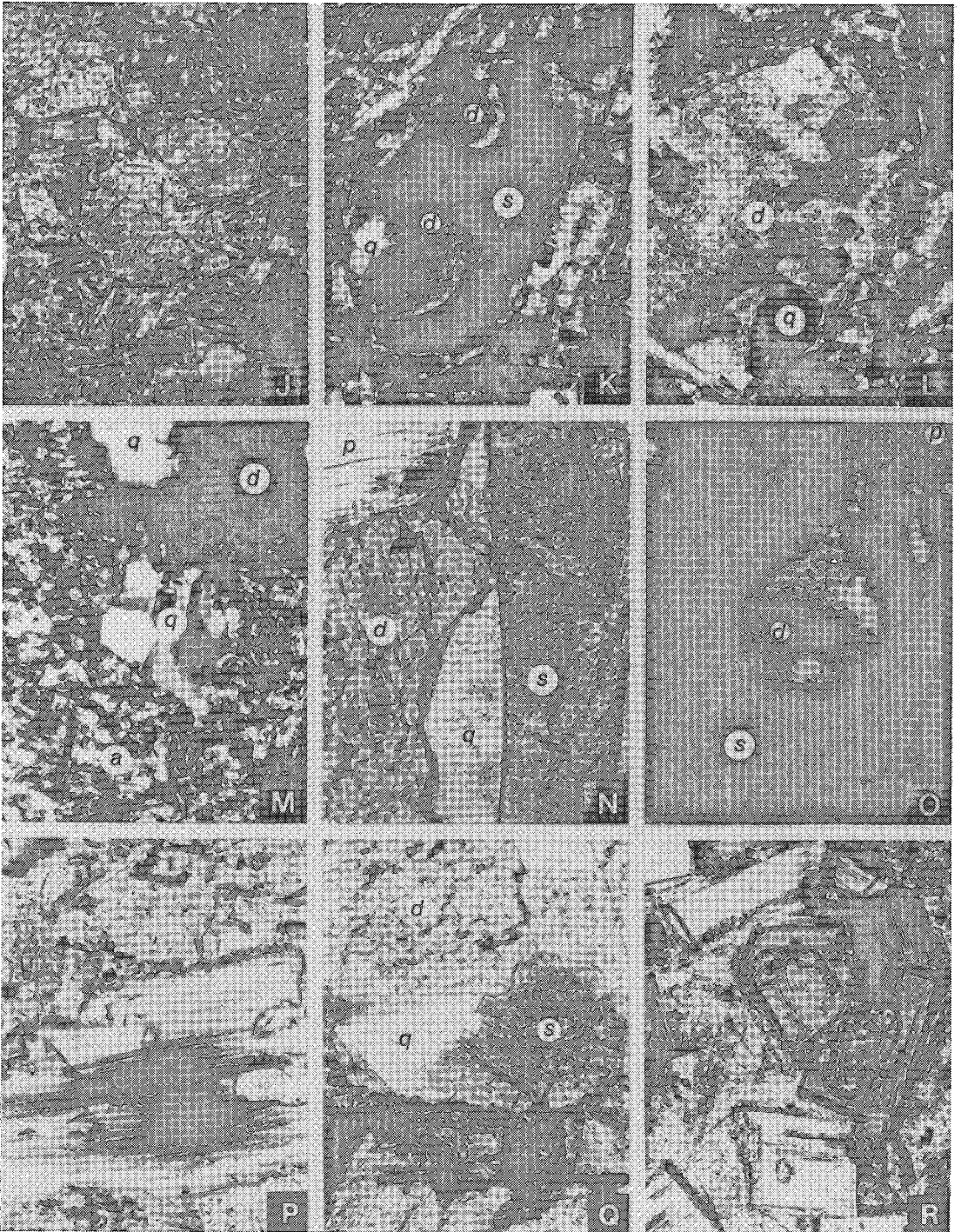


FIG. 2. Photomicrographs of the Concord minette. Long dimension of each photo is given in parentheses at the end of explanation. Minerals are labeled as follows: albite (a); calcite (c); dolomite (d); granular calcite pseudomorph after clinopyroxene (g); phlogopite (p); quartz (q); sanidine (s); and pseudomorph after olivine (x). J. FDO. Larger ocellus (center to left of center) has acicular phlogopite, cpx-pseudomorphs (small dark granules), and poorly developed phlogopite halo. Other ocellus (upper-right center) has well developed halo, a few cpx-pseudomorphs, and

The CDO are small (<2 mm) elliptical to polyhedral carbonate-mineral segregations with well developed phlogopite halos. Low sphericities and crinkled rims also suggest minor shrinkage (Fig. 2F, H, L). Fe-rich dolomite (49.5 Ca, 37.9 Mg, 12.2 Fe, 0.4 Mn atom %), the major mineral, occurs as single-crystal grains with mosaic subgrain textures (Spry 1969; Fig. 2L). Grains are mottled by structurally controlled dark (metal-rich?) patches (Fig. 2F). Clear low-Mg calcite (95.3 Ca, 0.7 Mg, 1.6 Fe; 2.4 Mn atom %) overgrows dolomite toward the interiors of the ocelli (Fig. 2F). Chlorite ($Mg^* = 0.7$) aggregates, siliceous pale green phlogopite, and pore space are commonly associated with calcite (Fig. 2H). Each ocellus has one or more mosaic-textured quartz crystals and smaller pyrite crystals that grew inward from the walls (Fig. 2F, L). Minor phases include fluorite, barite, celestine, anhydrite, very rare magnetite (96 mole % Fe_3O_4), chalcopyrite, and radiating clusters of acicular hematite (Fig. 2H). Angular, late-stage pores ($d < 2$ mm) were filled with mosaic-textured quartz (Fig. 2M). In the CDO and quartz-filled areas, rare spherulitic sanidine clumps exhibit clear, inclusion-free, rationally bounded overgrowths where they once projected into open pores (Fig. 2O).

PETROGENETIC HISTORY AND PHLOGOPITE COMPOSITIONS

Minette and other regional K-Ar ages (Table 1; Worthington & Lutz 1975, Kish as reported in McSween *et al.* 1984) indicate that the Concord-area rocks (Fig. 1) have remained relatively cool ($T < 300^\circ C$, the argon retention temperature of biotite) since the Early Devonian. The width of the dyke (0.5 m) and the inferred low wallrock temperatures suggest that the magma cooled and crystallized in one or two days (Szekely & Reitan 1971, Jaeger 1968). Cooling rates could easily have exceeded those that resulted in spherulitic crystallization of alkali feldspars under laboratory conditions (Lofgren 1971a). Use of a geothermal gradient during Early

Carboniferous time of $20^\circ C/km$, uniform erosion rates from 400 to 100 Ma ago, and the estimated emplacement depth (17 km) of the Concord plutonic complex about 400 Ma ago (Olsen *et al.* 1983, McSween *et al.* 1984) gives about 12 km as the emplacement depth for the Concord minette. This estimate is crude at best and ignores possible Carboniferous tectonic events in the region (Cook 1983, Ellwood 1982, Hatcher & Zietz 1980). I will suggest only that the Concord dyke was emplaced at upper crustal levels and that lithostatic pressures were probably 5 kbar or less.

Composition ($Mg^* fO_2, aH_2O$), T , and P affect Ti partitioning in phlogopite (Arima & Edgar 1981, Tronnes *et al.* 1985, Esperanca & Holloway 1986, 1987). Based on petrographic observations and the above-cited experimental data, Ti contents of the various Concord phlogopites (Fig. 4) are interpreted to suggest that phenocryst growth at high P was followed by initial growth of *in situ* matrix crystals at low P with only minor changes in temperature and

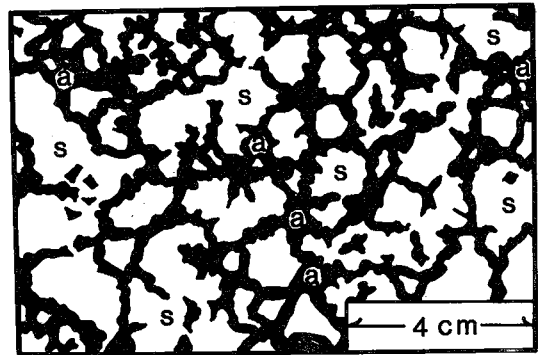


FIG. 3. Textural relationship of sanidine and albite in the Concord minette. Clear areas (s) represent long-fiber spherulitic sanidine. The sanidine grew first, so the later crystallizing albite occupies an interstitial position between the sanidine spherulites. This figure was traced from the surface of a sawed slab.

no acicular phlogopite. Feldspar is spherulitic sanidine (6.9 mm). K. CDO inside FDO. FDO has elliptical cross-section; CDO are circular (1.2 mm). L. Mosaic subgrain texture of dolomite in CDO. Subgrain units differ in extinction by $< 2^\circ$. Halo phlogopite has dark biotite overgrowth on matrix side and light-colored celadonic phlogopite or chlorite overgrown on the ocellus side (1.2 mm). M. Mosaic subgrain texture of cavity-filling quartz. Subgrain units differ by $< 2^\circ$ in extinction. Note angular shape of original cavity, and compare habit of matrix albite to that of sanidine in Figures 2B and 2O (1.2 mm). N. Meniscus developed between carbonate-rich fluid and alkali feldspar-rich silicate glass. Sanidine is spherulitic (0.32 mm). O. CDO inside FDO. The spherulitic sanidine grew from silicate melt or glass that surrounded a carbonate-rich fluid bubble. Clear light- to dark-grey grains (right rim of CDO) are quartz (1.2 mm). P. Interior alteration zone in phlogopite phenocryst. Altered zones (nearly opaque) give typical phlogopite analyses but with slightly low totals (Table 2, anal. 3) (1.2 mm). Q. Rational overgrowths on spherulitic sanidine. Euhedral overgrowths (clear) developed on spherulitic sanidine that impinged into vapor-phase cavity (now filled by quartz). The sanidine, quartz, and dolomite are inside a CDO. Note the dark rim of the ocellus (lower third of photo) (0.5 mm). R. Portion of cognate xenolith (Harrisburg minette). Subhedral embayed phlogopite is set in a matrix of microgranophyric alkali feldspar (probably anorthoclase; microprobe analyses show substantial Ca) (0.32 mm).

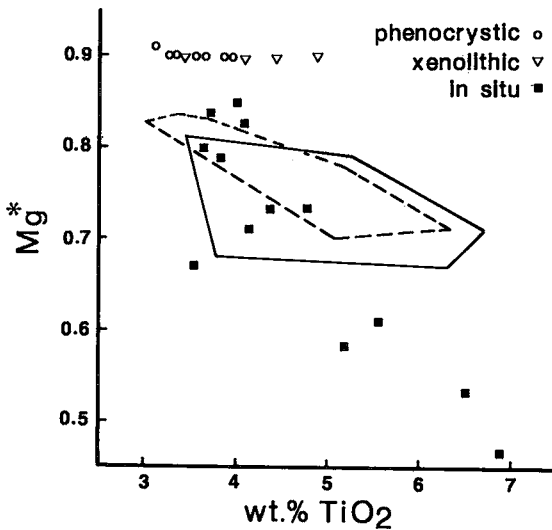


FIG. 4. Mg^* - TiO_2 distribution for phlogopite and biotite from the Concord minette. Polygons enclose data points for biotites (18) from the Camp Creek high-K latite grey phase (dashed lines) and for biotites (18) produced experimentally (solid lines) using the same grey latite as starting material (see Esperanca & Holloway 1986). In the Concord micas, TiO_2 variations are independent of Mg^* for $Mg^* > 0.75$; for $Mg^* < 0.75$, increasing TiO_2 correlates very closely with decreasing Mg^* , suggesting that $\ln D(Ti)$ values were increasing rapidly as the temperature fell and as the melt was enriched in Fe.

composition. The xenolithic phlogopite could have crystallized earlier at some intermediate depth. Anhydrous rutile occurs in the xenoliths, but rutile-coarse phlogopite aggregates have not been found. Thus rutile may not have crystallized together with the phlogopite phenocrysts.

Primary carbonates (no graphite), rutile, and late-stage hematite and sulfates suggest that the magma was relatively oxidizing ($>NNO$), but fO_2 variations are not known. The αH_2O probably remained consistently high. At depth, dissolved carbonates would have suppressed H_2O solubility in the melt, and in the dyke the magma was first oversaturated, then undersaturated, and finally oversaturated again as vapor-phase activity accompanied final solidification. Low Al_2O_3 contents (13–15%; Table 2) in phlogopite (Esperanca & Holloway 1986) are consistent with high αH_2O and with suppression of cpx-forming cation activities by dissolved carbonates. Clinopyroxene (now granular calcite pseudomorphs) began to crystallize only after most of the carbonates had exsolved from the dyke magma.

$\ln D(Ti)$ values (Esperanca & Holloway 1987) estimated for the Concord phlogopites (Fig. 5) and the near correspondence in Mg^* - TiO_2 distributions

between Concord matrix phlogopite (Fig. 4) and experimentally grown phlogopite (Esperanca & Holloway 1987) suggest similar T , fO_2 , and αH_2O in both situations. Thus $\ln D(Ti)$ values for the highest- Mg^* Concord matrix grains probably give reasonable minimum magma-emplacement temperatures (1050–1100°C). For the matrix flakes, the linear trend of increasing TiO_2 with decreasing Mg^* (Fig. 4) must have been controlled largely by decreasing T , increasing fO_2 and decreasing Mg^* .

The chemical zoning patterns in the phlogopite phenocrysts probably reflect variable magma composition in the deep-seated chamber. Chromium, Ni, Mg, and F were fractionated into the growing crystals while Ti, Ba, Fe, and probably OH increased in the residual magma. The chemical zonations indicate that the normal fractional crystallization trend was interrupted by injection of more primitive (high Mg and Cr) magma into the deep-seated chamber. Mixing and assimilation involving later more primitive magma and earlier partly crystallized minettes are to be expected since successive melt batches probably followed common pathways from the mantle into the deep-seated chamber and upper crust.

Under laboratory conditions, phlogopite kink bands anneal within a few hours at temperatures of 1050–1100°C (Etheridge & Hobbs 1974, Tullis 1976). The kinked phenocrysts in the Concord and Harrisburg minettes show absolutely no signs of annealing, suggesting that dyke emplacement followed soon after the crystals were deformed. Deformed aggregates of phlogopite, clinopyroxene, and apatite in the Harrisburg minettes suggest that a solidified or partly solidified minette was disaggregated and incorporated into the dyke-forming magma. Rapid evacuation and implosive collapse of a deep-seated, partly crystallized magma chamber may have provided enough energy to deform the phlogopite and to propel the minette rapidly into the upper crust. The crystal deformations could be due to shock (Borg 1972, Carter *et al.* 1986).

Catastrophic loss of a fluid phase (mainly CO_2) could have caused the implosion and provided enough energy to propagate a fissure system ahead of the rising magma (Anderson 1979). Rapid injection of more primitive magma into a partly solidified deep-seated chamber might also have triggered an eruption. However, low Cr contents in the matrix phlogopite suggest (Table 2, anal. 10) that prior to emplacement the dyke magma had already been depleted in Cr.

HOW DID THE FELDSPAR-DOMINANT OCELLI FORM?

The ocelli could represent any of the following features: (1) amygdules (Rock 1984); (2) crystallized droplets of immiscible liquid (Ferguson & Currie 1971, Philpotts 1972, 1976, Roedder 1979); (3)

spherulites (Carstens 1982); (4) pelletal lapilli or autoliths (Dawson 1980, Lorenz 1979); (5) crystallized drops of melted syenite wallrock; (6) segregation vesicles (Smith 1967, Roedder 1979, Cooper 1979); or (7) crystallized droplets of solute condensed from dense fluid-phase bubbles (Carmichael *et al.* 1974, Cooper 1979). The spherulitic sanidine in the ocelli indicates grain growth from a supercooled silicate melt or glass; thus the ocelli are not amygdules. Immiscibility between silica-oversaturated alkali feldspar-rich melt (the FDO) and a similar melt but with phlogopitic components in addition (minette groundmass) seems highly unlikely.

Phlogopite-free ocelli could develop through spherulitic crystallization if the alkali feldspars crystallized before the phlogopite. In the Concord minette, sanidine spherulitic fibers grew around the fine-grained phlogopite, showing clearly that the phlogopite crystallized first. Also, for the FDO to be spherulites, the fiber clumps should diverge outward, which is not the case.

Pelletal lapilli (rounded, elliptical, quenched magma drops occasionally with mica halos) are fairly common in upper diatreme zones of kimberlites (Lorenz 1979). They commonly have lithic nuclei and accretionary layering. None of these characteristics is evident in the FDO. Wallrock chips (90% alkali feldspars and minor biotite and clinopyroxene) might have melted to alkali feldspar-rich drops in the minette magma. However, the size and abundance distributions of the FDO are compatible with vesicle growth under a lateral thermal gradient. Such distributions would be highly unlikely for randomly-sized chips of wallrock. The melted-wallrock interpretation has other difficulties. Since phlogopite was crystallizing from the magma, it ought also to have grown as a rim around the melting chip; however, the largest ocelli have a poorly developed halo or lack one, whereas the smaller ocelli have a well-developed halo. In addition, a different mechanism would be needed to explain halos around the CDO.

Vesicles that are supposed to become filled or partly filled with late-stage interstitial melt (producing felsic ocelli in a more mafic host) are called segregation vesicles (Smith 1967). Although the vesicle-filling mechanism is controversial (Roedder 1979), most authors have assumed that the host rock was mechanically rigid, but not completely crystallized, when the vesicles were filled (Smith 1967, Upton & Wadsworth 1971, Van Wagoner 1983). The Concord FDO precursor vesicles were filled when the magma was still mainly liquid. Phlogopite crystals alone (30% by vol.) could not have provided mechanical rigidity in the dyke before the matrix (70% by vol.) crystallized. In fact, the Concord precursor vesicles formed, filled with silicate liquid, and disappeared before the matrix feldspars ever crystallized. Thus

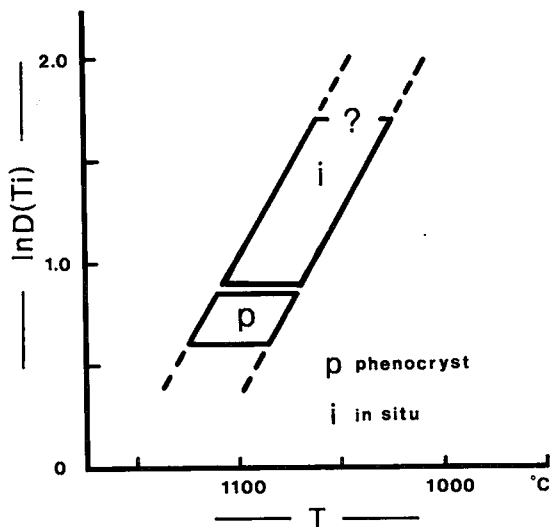


FIG. 5. Calculated $\ln D(\text{Ti})$ for Concord minette phlogopite. $D(\text{Ti})$ is wt.% TiO_2 in phlogopite divided by wt.% TiO_2 in melt. For phenocrysts TiO_2 (melt) was taken as the whole rock value (1.7%; Table 1, Mauer this issue); for *in situ* flakes, TiO_2 (melt) was estimated as 1.3% by subtracting the contribution of the phenocrysts (12 wt.% of rock; anal. 1, Table 2) from the total rock analysis. Heavy sloping lines enclose phenocrysts (11 analyses) and *in situ* flakes (13 analyses). Fe-rich mica values are too low because these grains were growing when TiO_2 (melt) was much less than 1.3 wt.%. Temperature $\ln D(\text{Ti})$ data from Esperanca & Holloway (1987).

the Concord FDO originated by a different mechanism.

ARE THE OCELLI CRYSTALLIZED CONDENSED FLUID-PHASE DROPLETS?

By default, this process is left as the only remaining possibility. However, some key assumptions need to be justified. (1) Decompression, caused by very rapid rise of the magma from lower crustal or upper mantle depths, can generate strong oversaturations in hydrous fluid-phase and carbonate-melt components. This assumption is appropriate for dissolved H_2O and probably for F; high pressures also probably raise carbonate solubilities in magmas with abundant alkalis and alkaline earths (Wendlandt & Harrison 1979, Freestone & Hamilton 1980). (2) Dissolved carbonates greatly suppressed the solubility of fluid components (OH and F) in the minette magma at depth so that with decompression, the magma was oversaturated with fluid-phase components but total fluids in the magma were still fairly low (<3 wt%). Experimental studies on other melt

compositions support this assumption for H₂O (Mysen 1976, 1983, Kadik & Lukanin 1973, Kadik *et al.* 1972). (3) The fluid-phase bubbles and carbonate-melt drops grew *in situ* in the dyke, but the fluid-phase bubbles grew much faster than the carbonate-melt droplets; later the volatiles (H₂O, F) redissolved in the dyke magma and the fluid-phase bubbles disappeared. *In situ* vesicle growth is demonstrated by the size and abundance distributions for the CDO and FDO. The ratio (*G*) of the two new phase growth rates may be modeled as follows:

$$G \propto (D_f^i/D_c^i) (\nabla\mu_i^{m,f}/\nabla\mu_i^{m,c})^n \quad n \geq 1$$

where *D_i* are diffusion matrices approximated by diffusivities (*f* fluid phase, *c* carbonate phase, and *m* melt phase) and the $\nabla\mu_i$ are chemical-potential gradients (Anderson & Buckley 1974, Cooper 1974) that depend on the chemical-potential differences between components in the melt and newly forming phases (initially for the fluid-phase and carbonate-phase components $\mu_i^m > \mu_i^f$ and $\mu_i^m > \mu_i^c$) and on diffusion lengths which were probably about the same for melt components diffusing toward both newly forming phases. Diffusivity data for basaltic and rhyolitic melts and ionic size and charge considerations (Hofmann 1980, Watson 1979, 1981, Delaney & Karsten 1981) suggest that coupled diffusivities for the fluid-phase components (K⁺, Na⁺, F⁻, and OH⁻) ought to have been three or more orders of magnitude larger than those for the carbonate-melt phase components (Ca²⁺, CO₃²⁻, Mg²⁺, and Fe²⁺). Only if $\nabla\mu_i^{m,c}$ greatly exceeds $\nabla\mu_i^{m,f}$ could the new-phase growth rates have been of the same order of magnitude. Thus the fluid-phase bubbles probably grew quickly when fluid-component solubilities were still suppressed by the dissolved carbonates. Later, after the exsolution of carbonates had gradually raised fluid solubilities, the direction of $\nabla\mu_i^{m,f}$ was reversed ($\mu_i^f > \mu_i^m$) and the fluid-phase volatiles redissolved in the magma or were incorporated into growing phlogopite.

The remaining assumptions (4) involve the physicochemical nature (density, composition, and solubilities for silicate melt components) of the precursor vesicle fluid, the volume ratio (*V_v/V_o*) of precursor vesicle to ocellus, and the change in dyke volume (ΔV) in response to changes in the fluid-phase volume. Calculations with appropriate values for the volume of ocelli in the dyke ($1 < V_o < 5\%$) and for the quantity of volatiles ($0.5 < \text{OH}^- + \text{F}^- < 3 \text{ wt.}\%$) in the magma give $V_v/V_o < 17$ and $\Delta V < 15\%$. Reducing OH⁻ plus F⁻ in the fluid phase to $< 2 \text{ wt.}\%$ of the magma further restricts Δ_v/V_o (< 8) and ΔV ($< 10\%$). The latter values for V_v/V_o and ΔV require high fluid-phase densities (> 0.5) and solubilities for silicates in excess of 25 wt.%; however excessive increases in dyke volume are eliminated.

The fluid phase was probably a dense, hydrous alkali fluoride solution whose existence and high solvent power under magmatic conditions have been inferred through fluid-inclusion studies (Roedder & Coombs 1967, Koster Van Groos & Wyllie 1968a, Lemlein *et al.* 1962). A temporary unstable solvus is suggested (Fig. 6, A-A') along which a silicate melt, strongly oversaturated in carbonates and fluid-phase components and low in total dissolved fluid-phase components, was in metastable equilibrium with a hydrous fluorine-bearing fluid phase rich in dissolved felsic melt components. This metastable solvus initially controlled the bulk composition of the fluid-phase bubbles. As the carbonates exsolved, the metastable solvus shifted toward a stable solvus along which a carbonate-saturated silicate melt was in equilibrium with the fluid phase (Fig. 6, C-C'). This shift produced rising fluid solubilities in the silicate melt and falling melt-component solubilities in the fluid phase. Declining temperatures enhanced those trends. When the fluid-phase bubbles disappeared, the melt components formerly dissolved in the bubbles were left as compositionally distinctive droplets that crystallized into the FDO as the dyke quickly cooled.

Rapid decompression and hydrous fluid and carbonate oversaturations may have produced a disrupted unstable melt structure. Diffusive fluxes imply instability since bonds between diffusing species and other melt species were rapidly breaking and forming. Due to the disequilibrium conditions, solubilities of the felsic melt components in the hydrous fluid may have been enhanced temporarily, helping to explain the initially high solubilities (A', Fig 6) and the transition to lower more normal solubilities (C', Fig. 6) as near-equilibrium conditions were established.

MATRIX AND CDO CRYSTALLIZATION AND VAPOR-PHASE ACTIVITY

The carbonate liquid droplets grew slowly as carbonate oversaturation declined and as diffusivities fell rapidly with declining temperature. The small high-Mg* phlogopite flakes then crystallized, followed by apatite and the Fe-rich phlogopite. The remaining felsic melt then crystallized. Sanidine spherulite fiber diameters suggest growth at $T < 550^\circ\text{C}$ (Lofgren 1971b); the nearly pure end-member feldspar compositions are consistent with low-temperature crystallization possibly in contact with a vapor phase. Vapor-phase activity accompanied and followed spherulitic crystallization; olivine and clinopyroxene were altered, rational overgrowths developed on spherulitic sanidine in pores, angular cavities filled with quartz, and the interior alteration zones in phlogopite phenocrysts may have formed. Hydrous alteration minerals, abundant quartz, and

minor fluorite suggest that the vapor phase was mainly H₂O (Luth & Tuttle 1969) with a minor fluorine component. Oxygen isotope results on calcite (+12‰) and dolomite (+8‰) argue against any influx of meteoric waters. Holding OH⁻ plus F⁻ to <2 wt.% of the magma implies that most of the volatiles were retained in the dyke. This assumption is supported by three observations. First, the late-stage minerals contain numerous volatiles, including easily lost species such as Cl. Secondly, wallrock permeabilities (the syenite is massive and unfractured; locally it is quarried as dimension stone) were probably very low, and thirdly, the minette has original open pores (3% porosity).

The immiscible carbonate-melt droplets (Eby 1980, Roedder 1979) crystallized more or less simultaneously with vapor-phase activity. Mosaic textures in quartz and dolomite and spherulitic textures in rare sanidine suggest rapid crystallization from a melt or dense fluid. These features and a lack of concentric internal patterns argue against the CDO being amygdules. Rare combined feldspar-carbonate ocelli probably originated when a fluid-phase bubble merged with a carbonate-melt droplet. Menisci between the carbonate-melt and vesicle-filling silicate liquid were occasionally preserved (Fig. 2N). The tiny CDO inside FDO (Fig. 2K, O) probably formed when an expanded fluid-phase bubble merged with a small carbonate-melt droplet. Isolated inside the fluid-phase bubble, the carbonate droplet stopped growing and was later enclosed by the condensed silicate solute from the bubble. Sanidine fiber growth patterns show that these small carbonate-melt droplets were embedded in the FDO before the silicate melt crystallized (Fig. 2O).

INTERPRETATION OF THE PHLOGOPITE HALOS

Halos associated with the CDO and smaller FDO exhibit similar characteristics. Halo flakes have {001} roughly tangential to the ocelli walls. Those surrounding FDO have biotite overgrowths on all sides. Flakes surrounding CDO have biotite overgrowths on sides that contacted silicate melt, but siliceous phlogopite or chlorite mantle the ocellus side (Fig. 2L).

Consider a fluid-phase bubble suspended in a magma. As the bubble volume changes by diffusion or pressure variation (Sparks 1978), the adjacent melt moves radially. Flow displacements decrease outward from the bubble surface, and suspended crystals would be expected to move with the melt. Thus a growing bubble would probably not accumulate nearby suspended crystals at the bubble-melt interface. However, crystals that nucleated and grew at the bubble-melt interface of an expanded vesicle would remain with the retreating interface as the bubble shrank.

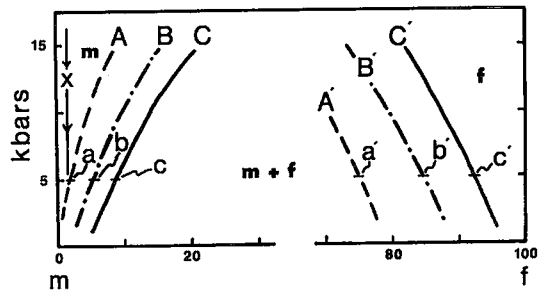


FIG. 6. Suggested magma and fluid-phase relationships for the Concord minette dyke. A-A' is a suggested solvus for the strongly carbonate-oversaturated magma, and the solvus B-B' corresponds to an intermediate degree of oversaturation. The melt-, melt-fluid-, and fluid-phase fields are designated by m, m + f, and f. Line x shows a decompression path corresponding to about 3 wt.% dissolved volatiles. At 5 kbars, melt (point a) with 3 wt.% dissolved volatiles would be in metastable equilibrium with fluid-phase bubbles containing about 25 wt.% dissolved melt components (point a'). As the carbonates exsolve, the solvus shifts to the right through B-B' toward C-C', raising fluid solubilities in the melt and lowering melt-phase component solubilities in the fluid phase (points c and c'). For dissolved volatiles >3 wt.% in the minette, decompression paths would intersect the solvus A-A' at pressures > 5 kbars; similar paths would intersect C-C' or some intermediate solvus at a more reasonable lower pressure, but the total volatile content of the magma would be excessive. A magma with substantially less than 3 wt.% dissolved volatiles would not vesiculate a fluid phase until the magma had reached very shallow depths even if the solvus A-A' was in control. Solubilities of melt components in the fluid bubbles along B' and C' are so low that the FDO could not have been derived from condensed solute unless the vesicles had shrunk substantially ($r_v/r_o > 2$); such highly expanded vesicles, however, imply an excessively large volume for the vesiculated magma in the dyke.

The mica halos probably originated through enhanced nucleation and crystal-growth rates in the bubble-melt interfacial zone. For phlogopite, nucleation successes and growth rates are assumed to have been controlled by the AlSi species and their mobilities in the melt (Kirkpatrick 1983, Dowty 1980). Thermal effects due to localized phase changes were probably inconsequential in such a rapidly cooling environment (Dowty 1980). The fluid-phase bubbles grew quickly before the matrix phlogopite began to crystallize. As the fluid-phase components redissolved, bridging oxygens were eliminated from the melt surrounding the bubble (Burnham 1979). Continued solution could have produced a less polymerized melt volume around the shrinking bubble in which the Al-Si species were more favorable for phlogopite nucleation and more mobile than in the bulk melt. Given equivalent degrees of undercool-

ing, nucleation successes and grain growth were enhanced in the interfacial zone. Nuclei with {001} tangential to the bubble wall were successful because their most rapidly growing edges were directed into the favorable zone; nuclei with other orientations could not grow into the bubble, and growth away from the bubble was inhibited by the unfavorable conditions in the bulk melt. In contrast, matrix flakes not associated with ocelli have random orientations, indicating that with additional undercooling, randomly oriented nuclei in the bulk melt grew successfully.

Water (dissolved as molecular H₂O; Freestone & Hamilton 1980, Koster Van Groos & Wyllie 1968b, Koster Van Groos 1975) expelled from the carbonate-melt droplets locally redissolved in the silicate melt, also enhancing selective growth of favorably oriented phlogopite nuclei. Precursor vesicles to the largest FDO opened in the hottest interior portions of the dyke where faster exsolution of carbonates promoted a rapid rise in solubilities of H₂O and F in the melt. Also, lateral thermal gradients and growth of matrix phlogopite in cooler marginal zones promoted localized losses of OH⁻ and F by diffusion. Thus these larger ocelli lack halos because their precursor vesicle fluids redissolved in the melt before the local matrix phlogopite flakes began to grow.

DISCUSSION: OCELLI AND SEGREGATION VESICLES

If silicate-rich ocelli form by the proposed condensed-solute mechanism, they ought to originate only in rapidly cooled H₂O- and carbonate-bearing magmas that rose directly into the upper crust from upper mantle or lower crustal depths. Silicate-rich and carbonate-rich ocelli and their associated phlogopite halos are direct evidence for the transient, strongly disequilibrium processes that accompanied rapid decompression and simultaneous oversaturations in carbonate and hydrous-fluid components. Ocelli and mafic mineral halos occur widely in minettes and other lamprophyres. Other more commonly occurring globular features, such as amygdules and spherulites, show no special preference for rocks crystallized or quenched from deep-seated, rapidly rising magmas.

Felsic ocelli in the common intermediate and mafic rocks are rare or absent except for segregation vesicles in deep-sea basalts (Van Wagoner 1983, Bideau *et al.* 1977, Sato 1978). Segregation vesicles are proposed to have originated by porous-media flow of late-stage, interstitial felsic liquid into vesicles in largely crystalline basalt (see discussions by Williams *et al.* 1982, p. 235, and Roedder 1979). High melt viscosity, low melt fraction, and tiny pore diameters combine to give very low permeabilities and flow velocities; steep pressure gradients are required to push the melt toward the vesicles. Assum-

ing 10 poise for interstitial-melt viscosity, a pore diameter of 1 mm, a melt fraction of 10%, and a flow velocity of 1 cm/hr give $\Delta P = 5.5$ bars/cm from Darcy's Law and the permeability equation of Von Bergen & Waff (1986). Lower flow velocities would allow for lower ΔP values, but more time would be required to fill the vesicles. In such a rapidly cooling environment, increasing viscosity and decreasing pore dimensions will cause porous-flow velocities to decrease rapidly with time. Lowered gas pressure in the vesicle has been proposed as the mechanism to generate ΔP . For the porous media to be permeable, the interstitial melt must be interconnected so that equalized gas pressures would result. Growing interstitial gas bubbles could force some liquid toward a lower pressure vesicle, but the origin of such bubbles remains a mystery.

Segregation vesicles may form by the condensed vapor-phase solute mechanism. The proposed requirements are generally satisfied; in particular, CO₂ is evidently an abundant volatile in these basalts. The early hydrous fluid-phase solute would be enriched in felsic components dissolved from the basalt magma; slower exsolution of CO₂ would increase H₂O solubilities in the melt while melt-phase components would be less soluble in the fluid phase as the CO₂/(CO₂ + H₂O) rose in the vesicle. With rapid cooling, the fluid-phase solute could be preserved as felsic glass that partly fills a vesicle.

ACKNOWLEDGEMENTS

Sharon Bachinski, A.F. Cooper, and two anonymous reviewers offered very important comments on earlier versions of the manuscript, and Todd Solberg helped the author learn how to operate the electron microprobe at VPI & SU. Funding was provided by the East Carolina University Research Committee.

REFERENCES

- ANDERSON, D.E. & BUCKLEY, G.R. (1974): Modeling of diffusion controlled properties of silicates. *In* Geochemical Transport and Kinetics (A.W. Hofmann, B.J. Giletti, H.S. Yoder, Jr. & R.A. Yund, eds.). *Carnegie Inst. Wash. Pub.* 634, 31-52.
- ANDERSON, O.L. (1979): The role of fracture dynamics in kimberlite pipe formation. *In* Kimberlites, Diatremes, and Diamonds: Their Geology, Petrology and Geochemistry. (F.R. Boyd & H.O.A. Meyer, eds.). Amer. Geophys. Union, Washington, DC, 344-352.
- ARIMA, M. & EDGAR, A.D. (1981): Substitution mechanisms and solubility of titanium in phlogopites from rocks of probable mantle origin. *Contr. Mineral. Petrology* 77, 288-295.

- BACHINSKI, S.W. & SIMPSON, E.L. (1984): Ti-phlogopite of the Shaw's Cove minette: a comparison with micas of other lamprophyres, potassic rocks, kimberlites, and mantle xenoliths. *Amer. Mineral.* **69**, 41-56.
- BELL, H. & OVERSTREET, W.C. (1959): Relations among some dikes in Cabarras County, North Carolina. *Geologic Notes 3 (no. 2), South Carolina Geol. Surv. (Columbia, SC)*, 1-5.
- BIDEAU, D., HEKINIAN, R. & FRANCHETEAU, J. (1977): Orientation of ocean floor basaltic rocks at the time of cooling: a general method. *Contr. Mineral. Petrology* **65**, 19-28.
- BORG, I.Y. (1972): Some shock effects in granodiorite to 270 kilobars at the Pile Driver site. *In Flow and Fracture in Rocks. Geophysical Monograph 16*, Amer. Geophys. Union, Washington, DC, 293-311.
- BURNHAM, C.W. (1979): The importance of volatile constituents. *In The Evolution of the Igneous Rocks: Fiftieth Anniversary Perspectives (H.S. Yoder, Jr., ed.)*. Princeton Univ. Press, Princeton, NJ, 437-482.
- CARMICHAEL, I.S.E., TURNER, F.J. & VERHOOGEN, J. (1974): *Igneous Petrology*. McGraw-Hill, New York, NY.
- CARTER, N.L., OFFICER, C.B., CHESNER, C.A. & ROSE, W.I. (1986): Dynamic deformation of volcanic ejecta from the Toba caldera: possible relevance to Cretaceous/Tertiary boundary phenomena. *Geology* **14**, 380-383.
- CARSTENS, H. (1982): Spherulitic crystallization in lamprophyric magmas and the origin of ocelli. *Nature* **297**, 493-494.
- COOK, F.A. (1983): Some consequences of palinspastic reconstruction in the southern Appalachians. *Geology* **11**, 86-89.
- COOPER, A.F. (1979): Petrology of ocellar lamprophyres from western Otago, New Zealand. *J. Petrology* **20**, 139-163.
- COOPER, A.R., Jr. (1974): Vector space treatment of multicomponent diffusion. *In Geochemical Transport and Kinetics (A.W. Hofmann, B.J. Gilletti, H.S. Yoder, Jr. & R.A. Yund, eds.)*. *Carnegie Inst. Wash. Pub.* **634**, 15-30.
- DAWSON, J.B. (1980): *Kimberlites and Their Xenoliths*. Springer-Verlag, Berlin.
- DELANEY, J.R. & KARSTEN, J.L. (1981): Ion microprobe studies of water in silicate melt; concentration dependent water diffusion in obsidian. *Earth Planet. Sci. Lett.* **52**, 191-202.
- DOWTY, E. (1980): Crystal growth and nucleation theory and the numerical simulation of igneous crystallization. *In Physics of Magmatic Processes (R.B. Hargraves, ed.)*. Princeton Univ. Press, Princeton, NJ, 419-486.
- EBY, G.N. (1980): Minor and trace element partitioning between immiscible ocelli-matrix pairs from lamprophyre dikes and sills, Montereian Hills petrographic province, Quebec. *Contr. Mineral. Petrology* **75**, 269-278.
- EHRENBERG, S.N. (1979): Garnetiferous inclusions in minette from the Navajo Field. *In The Mantle Sample: Inclusions in Kimberlite and other Volcanics (F.R. Boyd & H.O.A. Meyer, eds.)*. Amer. Geophys. Union, Washington, DC, 330-334.
- ELLWOOD, B.B. (1982): Paleomagnetic evidence for the continuity and independent movement of a distinct major crustal block in the Southern Appalachians. *J. Geophys. Res.* **87**, 5339-5350.
- ESPERANCA, S. & HOLLOWAY, J.R. (1986): The origin of the high-K latites from Camp Creek, Arizona: constraints from experiments with variable fO_2 and aH_2O . *Contr. Mineral. Petrology* **93**, 504-512.
- _____ & _____ (1987): On the origin of some mica lamprophyres: experimental evidence from a mafic minette. *Contr. Mineral. Petrology* **95**, 207-216.
- ETHERIDGE, M.A. & HOBBS, B.E. (1974): Chemical and deformational controls on recrystallization of mica. *Contr. Mineral. Petrology* **43**, 111-124.
- FARMER, G.L. & BOETTCHER, A.L. (1981): Petrologic and crystal-chemical significance of some deep-seated phlogopites. *Amer. Mineral.* **66**, 1154-1163.
- FERGUSON, J. & CURRIE, K.L. (1971): Evidence of liquid immiscibility in alkaline ultrabasic dykes at Callender Bay, Ontario. *J. Petrology* **12**, 561-585.
- FREESTONE, I.C. & HAMILTON, D.L. (1980): The role of liquid immiscibility in the genesis of carbonatites; an experimental study. *Contr. Mineral. Petrology* **73**, 105-117.
- GOLDSMITH, R., MILTON, D.F. & WILSON, F.A. (1978): Preliminary geologic map, geologic map index, and annotated bibliography, Charlotte 2° sheet, North Carolina and South Carolina. *U.S. Geol. Surv. Open-File Map 78-590*.
- HATCHER, R.D., Jr. & ZIETZ, I. (1980): Tectonic implications of regional aeromagnetic and gravity data from the Southern Appalachians. *In The Caledonides in the USA (D.R. Wones, ed.)*. *Virginia Polytech. Inst. State Univ., Dep. Geol. Sci., Mem.* **2**, Blacksburg, VA, 235-244.
- HOFMANN, A.W. (1980): Diffusion in natural silicate melts: a critical review. *In Physics of Magmatic Processes (R.B. Hargraves, ed.)*. Princeton Univ. Press, Princeton, NJ, 385-417.

- JAEGER, J.C. (1968): Cooling and solidification of igneous rocks. In Basalts. The Poldervaart Treatise on Rocks of Basaltic Composition (H.H. Hess & A. Poldervaart, eds.). Wiley-Interscience, New York, NY, 503-536.
- KADIK, A.A. & LUKANIN, O.A. (1973): The solubility dependent behavior of water and carbon dioxide in magmatic processes. *Geochem. Int.* **10**, 115-129.
- _____, _____, LUBEDEV, YE. B. & KOROVUSHINA, E. YE. (1972): Solubility of H₂O and CO₂ in granite and basalt. *Geochem. Int.* **9**, 1041-1050.
- KIRKPATRICK, R.J. (1983): Theory of nucleation in silicate melts. *Amer. Mineral.* **68**, 66-77.
- KOSTER VAN GROOS, A.F. (1975): The effect of high CO₂ pressures on alkalic rocks and its bearing on the formation of alkalic ultrabasic rocks and the associated carbonatites. *Amer. J. Sci.* **275**, 163-185.
- _____ & WYLLIE, P.J. (1968a): Melting relationships in the system NaAlSi₃O₈-NaF-H₂O to 4 kilobars pressure. *J. Geology* **76**, 50-70.
- _____ & _____ (1968b): Liquid immiscibility in the join NaAlSi₃O₈-Na₂CO₃-H₂O and its bearing on the genesis of carbonatites. *Amer. J. Sci.* **266**, 932-967.
- LECHEMINANT, A.N. & LECHEMINANT, G.M. (1985): Phlogopite from 1.8 Ga lamprophyres and trachyandesites, district of Keewatin: petrological implications. *Prog. Abstr., Geol. Assoc. Can./Mineral. Assoc. Can.* **10**, A33.
- LEMMLEIN, G.G., KLIYA, M.O. & OSTROVSKII, I.A. (1962): The conditions for formation of minerals in pegmatites according to primary inclusions in topaz. *Soviet Phys. Dokl.* **7**, 4-6.
- LOFGREN, G.E. (1971a): Experimentally produced divitrification textures in natural rhyolite glass. *Geol. Soc. Amer. Bull.* **82**, 111-124.
- _____ (1971b): Spherulitic textures in glassy and crystalline rocks. *J. Geophys. Res.* **76**, 5635-5648.
- LORENZ, V. (1979): Phreatomagmatic origin of the olive mellite diatremes of the Swabian Alb, Germany. In Kimberlites, Diatremes, and Diamonds: Their Geology, Petrology, and Geochemistry (F.R. Boyd & H.O.A. Meyer, eds.). Amer. Geophys. Union, Washington, DC, 354-363.
- LUTH, W.C. & TUTTLE, O.F. (1969): The hydrous vapor phase in equilibrium with granite and granite magmas. *Geol. Soc. Amer. Mem.* **115**, 513-548.
- MCSWEEN, H.Y., JR., SANDO, T.W., CLARK, S.R., HARDEN, J.T. & STRANGE, E.A. (1984): The gabbro-metagabbro association of the southern Appalachian Piedmont. *Amer. J. Sci.* **284**, 437-461.
- MERCIER, J.-C. (1979): Peridotite xenoliths and the dynamics of kimberlite intrusion. In The Mantle Sample: Inclusions in Kimberlites and other Volcanics (F.R. Boyd & H.O.A. Meyer, eds.). Amer. Geophys. Union, Washington, DC, 197-212.
- MYSEN, B.O. (1976): The role of volatiles in silicate melts: solubility of carbon dioxide and water in feldspar, pyroxene, and feldspathoidal melts to 30 kb and 1625°C. *Amer. J. Sci.* **276**, 969-996.
- _____ (1983): The solubility mechanisms of volatiles in silicate melts and their relations to crystal-andesite liquid equilibria. *J. Volcanological Geotherm. Res.* **18**, 361-385.
- NICOLAS, A. & POIRIER, J.P. (1976): *Crystalline Plasticity and Solid State Flow in Metamorphic Rocks*. John Wiley & Sons, New York, NY.
- OLSEN, B.A., MCSWEEN, H.Y., JR. & SANDO, T.W. (1983): Petrogenesis of the Concord gabbro-syenite complex, North Carolina. *Amer. Mineral.* **68**, 315-333.
- PHILPOTTS, A.R. (1972): Density, surface tension and viscosity of the immiscible phase in a basic alkaline magma. *Lithos* **5**, 1-18.
- _____ (1976): Silicate liquid immiscibility; its probable extent and petrogenetic significance. *Amer. J. Sci.* **276**, 1147-1177.
- PHILLIPS, W.J. (1973): Interpretation of crystalline spheroidal structures in igneous rocks. *Lithos* **6**, 235-244.
- READ, H.H. (1926): The mica lamprophyres of Wigtownshire. *Geol. Mag.* **63**, 422-429.
- REYNOLDS, D.L. (1931): The dykes of the Ards peninsula, County Down. *Geol. Mag.* **68**, 97-111 & 145-165.
- ROCK, N.M.S. (1984): Nature and origin of calc-alkaline lamprophyres: minettes, vogesites, kersantites and spessartites. *Roy. Soc. Edinburgh Trans., Earth Sci.* **74**, 193-227.
- RODEN, M.F. & SMITH, D. (1979): Field geology, chemistry, and petrology of Buell Park minette diatreme, Apache County, Arizona. In Kimberlites, Diatremes, and Diamonds: Their Geology, Petrology and Geochemistry (F.R. Boyd & H.O.A. Meyer, eds.). Amer. Geophys. Union, Washington, DC, 364-381.
- ROEDDER, E. (1979): Silicate liquid immiscibility in magmas. In The Evolution of Igneous Rocks: Fiftieth Anniversary Perspectives (H.S. Yoder, Jr., ed.). Princeton Univ. Press, Princeton, NJ, 15-57.
- _____ & COOMBS, D.S. (1967): Immiscibility in gra-

- nitic melts indicated by fluid inclusions in ejected granitic blocks from Ascension Island. *J. Petrology* **8**, 417-451.
- SATO, H. (1978): Segregation vesicles and immiscible liquid droplets in ocean-floor basalts of hole 396B, IDOP/DSDP leg 46. *Initial Report, Deep Sea Drill. Project 46*, 283-291.
- SMITH, R.E. (1967): Segregation vesicles in basaltic lava. *Amer. J. Sci.* **265**, 696-713.
- SOLBERG, T.N. & SPEER, J.A. (1982): QALL, a 16-element analytical scheme for efficient petrologic work on an automated ARL-SEM: application to mica reference samples. In *Microbeam Analysis*, (K.F.J. Heinrich, ed.). San Francisco Press Inc., Box 6800, San Francisco, CA.
- SPARKS, R.S.J. (1978): The dynamics of bubble formation and growth in magmas: a review and analysis. *J. Volcanological Geotherm. Res.* **3**, 1-37.
- SPRY, A. (1969): *Metamorphic Textures*. Pergamon Press, Oxford, New York & Toronto.
- SZEKELY, J. & REITAN, P.H. (1971): Dike filling by magma intrusion and by explosive entrainment of fragments. *J. Geophys. Res.* **76**, 2602-2609.
- TRONNES, R.G., EDGAR, A.D. & ARIMA, M. (1985): A high pressure-high temperature study of TiO₂ solubility in Mg-rich phlogopite: implications to phlogopite chemistry. *Geochim. Cosmochim. Acta* **49**, 2323-2329.
- TULLIS, T.E. (1976): Experiments on the origin of slaty cleavage and schistosity. *Geol. Soc. Amer. Bull.* **87**, 745-753.
- UPTON, B.G.J. & WADSWORTH, W.J. (1971): Rhyodacite glass in Reunion basalt. *Mineral. Mag.* **38**, 152-159.
- VAN WAGONER, N.A. (1983): Critical evaluation of segregation vesicles in mid-ocean ridge basalts as a rock orientation tool. *J. Geophys. Res.* **88**, B10, 8318-8332.
- VON BARGEN, N. & WAFF, H.S. (1986): Permeabilities, interfacial areas, and curvatures of partially molten systems: results of numerical computations of equilibrium microstructures. *J. Geophys. Res.* **91**, B9, 9261-9276.
- WATSON, E.B. (1979): Calcium diffusion in a simple silicate melt to 30 kbar. *Geochim. Cosmochim. Acta* **43**, 313-322.
- _____ (1981): Diffusion in magmas at depth in the Earth: the effects of pressure and dissolved H₂O. *Earth Planet. Sci. Lett.* **52**, 291-301.
- WENDLANDT, R.F. & HARRISON, W.J. (1979): Rare earth partitioning between immiscible carbonate and silicate liquids and CO₂ vapor: results and implications for the formation of light rare earth-enriched rocks. *Contr. Mineral. Petrology* **69**, 409-419.
- WILLIAMS, H., TURNER, F.J. & GILBERT, C.M. (1982): *Petrography—An Introduction to the Study of Rocks in Thin Section (2nd ed.)*. W.H. Freeman and Co., San Francisco, CA.
- WORTHINGTON, H.D. & LUTZ, N.R. (1975): Porphyry copper-molybdenum mineralization at the Newell Prospect, Cabarrus County, North Carolina. *Southeastern Geology* **17**, 1-14.
- WRIGHT, T.L. (1968): X-ray and optical study of alkali feldspar II. An X-ray method for determining the composition and structural state from measurement of 2θ values for three reflections. *Amer. Mineral.* **53**, 88-104.

Received February 18, 1987; revised manuscript accepted October 13, 1987.